Aalborg Universitet

AALBORG UNIVERSITY

Coordinated Power Dispatch of a PMSG based Wind Farm for Output Power Maximizing Considering the Wake Effect and Losses

Zhang, Baohua; Hu, Weihao; Hou, Peng; Soltani, Mohsen; Chen, Zhe

Coordinated Power Dispatch of a PMSG based Wind Farm for Output Power Maximizing Considering the Wake Effect and Losses

Baohua Zhang, Weihao Hu, Peng Hou, Mohsen Soltani, Zhe Chen

Department of Energy Technology
Aalborg University
Aalborg, Denmark
bzh@et.aau.dk, whu@et.aau.dk, pho@et.aau.dk, sms@et.aau.dk, zch@et.aau.dk

Abstract—**The energy loss in a wind farm (WF) caused by wake interaction between wind turbines (WTs) is quite high, which can be reduced by proper active power dispatch. The electrical loss inside a WF by improper active power and reactive power dispatch is also considerable. In this paper, a coordinated active power and reactive power dispatch strategy is proposed for a Permanent magnet synchronous generator (PMSG) based WF, in order to maximize the total output power by reducing the wake effect and losses inside the devices of the WF, including the copper loss and iron loss of PMSGs, losses inside converters and transformers of WTs and the losses along the transmission cables. The active power reference and reactive power reference of each WT are chosen as the optimization variables and a partial swarm optimizing (PSO) algorithm is used for solving the problem. The proposed strategy is compared with traditional strategies in a designed WF. Simulation results show the effectiveness of the proposed strategy.**

Keywords—wind farm coordinated power dispatch; energy maximizing; wake effect; loss minimizing; PMSG

I. INTRODUCTION

Wake effect in a wind farm (WF) can cause a high level of energy loss, the study in [1] reports an average energy loss of 12% in an offshore WF caused by the wake. There are two types of wake control method for a WF: redirecting the wakes by yaw control [2-5] and reducing wake interaction by adjusting the axial induction [6-14]. The first method is studied in [2-4] and recently developed by the work in [5], where a control-oriented wake model called FLORIS is proposed. Most of the research works focus on the second method. These works maximize the total captured power of WFs by optimizing the control settings to each WT. The control variables are chosen as the axial induction factors [6], [7] the yaw offset angle, the thrust coefficient [8], the pitch angle [9], the rotational speed (tip speed ratio), or the combination of two of them as the control variables [10-13]. However, WT derating control strategy was not properly considered in these works. In [14], the active power reference of each WT is chosen as the optimization variable, and a Max-Ω WT control strategy proposed in [15] is adopted for derating control. Choosing the active power reference as the control variables is more suitable for the optimal power flow problems in power system engineering.

Besides the energy loss caused by wake effect, the electrical loss inside a WF is also considerable. The electrical losses inside the devices in a WF are related to the active and reactive power flows, which can be controlled by the WF controller or WT controllers. At the WF control level, the dispatch strategies which are used to distribute the demanded active and reactive power will decide the total losses. Proportional dispatch is a commonly used dispatch strategy for active power or reactive power [16-18]. This method is easy to implement and is unlikely to exceed the power limit of each WT. However, it cannot assure a high efficiency of the system. An optimal dispatch strategy for the reactive power is proposed in [19, 20], which includes the losses along the transmission cables and the transformers on WTs into the objective function. However, losses in the WT energy conversion systems were not considered. In [21], losses from wind energy conversion systems were included into the optimization, and an optimal dispatch of reactive power is proposed for total loss minimization. The above strategies only focus on active power dispatch or reactive power dispatch. However, the active power and reactive power are also related by the current and voltage limits of the WT energy conversion systems, so they should be considered together. The combined solution was proposed in [22, 23], where active and reactive power dispatch were optimized together mainly to minimize the electrical power losses in the transmission system.

Most of these works only focus on minimizing the energy loss caused by wakes or minimizing the electrical loss caused by power flows. In [14], these two objectives were combined together to realize an optimized active power dispatch, but only the electrical losses in the transmission cables were considered. However, the electrical losses inside the wind energy generation systems are higher. For a Permanent magnet synchronous generator (PMSG) based WT, which is becoming popular in wind turbine applications, the electrical losses

include the copper loss and iron loss of PMSGs, losses inside the converters and losses in the transformers.

In this paper, a coordinated active power and reactive power dispatch strategy is proposed for a PMSG based WF, which combined the purpose of minimizing the energy loss caused by wake effects and the purpose of minimizing the electrical losses caused by power flows. The electrical losses include not only the losses along the transmission system, but also the losses inside the energy conversion systems. The models of WTs, wakes and device losses are given and the optimization problem is formulated and solved by partial swarm optimizing (PSO). The proposed strategy is compared with traditional strategies in a designed WF. Simulation results show the effectiveness of the proposed strategy.

This paper is organized as follows: Section II describes the WF model. Section III shows the formulation of the optimization problem and the solving method. The simulation results of proposed strategy are given and discussed in Section IV, and finally conclusions are drawn in Section V.

II. WIND FARM MODEL

The wake model and the power loss model on transmission cables are specified in this section. The WT model using traditional control strategy with no derating is also illustrated and will be used as a baseline for comparison.

A. Wind Turbine Model

The WT can be described using a static model, which is based on the look-up tables of the power coefficient $C_P(\beta, \lambda)$ and the thrust coefficient $C_T(\beta, \lambda)$. Then, the WT mechanical power P_{mec} can be calculated using [24],

$$P_{mec} = \frac{\pi}{2} \rho R^2 v^3 C_p(\beta, \lambda) \quad (1)$$

where ρ is the air density, R is the rotor radius, v is the wind speed, β is the blade pitch angle and λ is the tip-speed ratio, which can be expressed by

$$\lambda = \omega R / v, \quad (2)$$

where ω is the rotor rotational speed.

The control strategy decides the steady state values of β and ω under a certain v, thus deciding the λ, and C_P and C_T then. The normal control of WT in the whole wind speed region can be divided into five regions, more details can refer to [26]. However, under derating operation, the control strategies need to be modified. In derating operation, the control target is to maintain the captured power at a reference value, usually lower than the available power. The WT normally uses torque control to regulate the power captured by the rotor, which increases the rotational speed. After the rotational speed is beyond its limits, the WT keeps the rotational speed at its limit and turns to pitch control.

B. Wake Model

The wake models can describe the aerodynamic interaction between WTs in the WF. The multiple wake model based on Jensen model is a common model to simulate the wakes, which can be expressed in the following equations [27], [28]:

$$v_{ij} = v_0 - v_0 * \left(1 - \sqrt{1 - C_t}\right) * \left(\frac{R_0}{R_{ij}}\right)^2 * \left(\frac{S_{overlap,ij}}{S_0}\right) \quad (3)$$

$$R_{ij} = R_0 + k * L_{ij}. \quad (4)$$

All the parameters have the same meaning as in the references. The wind velocity at the WT at row n, column m can be derived as:

$$v_{nm} = v_{0*}[1 - \sqrt{\sum_{i=1}^{N\_row} \sum_{j=1}^{N\_col} [1 - \left(\frac{v_{ij}}{v_0}\right)]^2}] \quad (5)$$

C. PMSG Loss Model

The steady state model of the surface-mounted PMSG in the magnet flux reference frame can be expressed as [29]:

$$\begin{aligned} u_{sd} &= -R_s i_{sd} + L_s \omega i_{sq} \\ u_{sq} &= -R_s i_{sq} - L_s \omega i_{sd} + \omega \psi \end{aligned} \quad (6)$$

Where R_s and L_s are the generator resistance and inductance respectively, ω is the generator rotational speed, and ψ is the amplitude of the flux induced by the permanent magnets of the rotor in the stator phases. The electromagnetic torque can be given by [29]

$$T_e = \frac{3}{2} p \psi i_{sq} \quad (7)$$

where p is the number of pole pairs. The q-axis current is proportional to the generator torque. The d-axis current is controlled to be zero to maximize the torque [30]. The copper loss can be calculated using

$$P_{Cu} = 3 R_s |I_s|^2 \quad (8)$$

Where R_s is the armature phase resistance and $|I_s|$ is the RMS magnitude of the phase current. And the iron losses is calculated using the relation [30]

$$P_{Fe} = k_1 \omega_{el}^2 \quad (9)$$

Where ω_{el} is the electrical speed of the machine and k_1 is a constant extracted from the iron losses at rated speed, and is found to be 0.1 [30].

D. Converter Loss Model

The losses in the converter, which consists of transistors and reverse diodes, can be divided into switching losses and conducting losses [31]. According to [31], the losses in a converter can be expressed as

$$P_{con} = a_l I_{rms} + b_l I_{rms}^2 \quad (10)$$

where I_{rms} is the rms value of the sinusoidal current at the converter ac terminal, and a_l and b_l are the power module constants and can be expressed as

$$a_l = \frac{6\sqrt{2}}{\pi}\left(V_{IGBT} + \frac{E_{ON} + E_{OFF}}{I_{C,nom}} f_{sw} + \frac{E_{rr}}{I_{C,nom}} f_{sw} \right) \quad (11)$$

$$b_l = 3r_{IGBT} \quad (12)$$

where V_{IGBT} is the voltage across the collector and emitter of the IGBT, $E_{ON} + E_{OFF}$ is the total turn-on and turn-off losses of the IGBTs, $I_{C,nom}$ is the nominal collector current of the IGBT, f_{sw} is the switching frequency, E_{rr} is the turn-off (reverse recovery) loss of the diodes, r_{IGBT} is the lead resistance of the IGBT.

E. Transformer Loss Model

The active power loss in transformers can be calculated using [32]

$$P_{trans} = P_0 + \alpha^2 P_k \quad (13)$$

where α is the load ratio, P_0 is the no-load loss, and P_k is the load loss.

F. Cable Loss Model

For a cable connecting two buses i and j, the cable current, I_{ij}, measured at bus i and j and defined positive in the direction $i \rightarrow j$ is given by [33]

$$I_{ij} = I_l + I_{i0} = y_{ij}\left(V_i - V_j\right) + y_{i0}V_i , \quad (14)$$

where y and I mean the admittance and current of each cable, and V means the voltage on each bus. Similarly, the cable current I_{ji} is given by

$$I_{ji} = -I_l + I_{j0} = y_{ij}\left(V_j - V_i\right) + y_{j0}V_j . \quad (15)$$

The power loss in cable ij is the algebraic sum of the complex powers S_{ij} from bus i and j and S_{ji} from bus j and i,

$$S_{ij}^{loss} = S_{ij} + S_{ji} = V_i I_{ij}^* + V_j I_{ji}^* . \quad (16)$$

III.   PROBLEM FORMULATION AND OPTIMIZATION

The optimization problem including the objective function and constraints are formulated and is solved by an improved PSO algorithm in this section.

The output active power of the WF can be calculated by:

$$P_{out}^{WF} = \sum_{k=1}^{N_W}\left(P_{mec}^k - P_{Cu}^k - P_{Fe}^k - P_{con}^k - P_{trans}^k \right) - \sum_{i=1,j=1}^{N_B} P_{ij}^{loss} \quad (17)$$

where P_{mec}^k, P_{Cu}^k, P_{Fe}^k, P_{con}^k, and P_{trans}^k are the captured power, copper loss, iron loss, losses of converters and transformer loss from WT k, respectively, N_W is the number of WTs, P_{ij}^{loss} is the active power loss in cable ij, N_B is the number of buses.

The reactive power at the PCC of the WF is expressed by:

$$Q_{PCC} = \sum_{k=1}^{N_W}Q_{ref}^k - \sum_{i=1,j=1}^{N_B} Q_{ij}^{loss}$$

where Q_{ref}^k is the reference reactive power of WT k and Q_{ij}^{loss} is the active power loss in cable.

Then, the optimization problem can be expressed as:

Objective: $\displaystyle \max_{P_{ref}^k, Q_{ref}^k}\ P_{out}^{WF}$ (18)

Constraints:

$$P_j = \left|V_j\right|\sum_{i=1}^{N_B}\left|V_i\right|\left|Y_{ji}\right|\cos\left(\theta_{ji} - \delta_j + \delta_i\right) \quad (19)$$

$$Q_j = -\left|V_j\right|\sum_{i=1}^{N_B}\left|V_i\right|\left|Y_{ji}\right|\sin\left(\theta_{ji} - \delta_j + \delta_i\right) \quad (20)$$

$$Q_{PCC} = Q_{ref}^{WF} \quad (21)$$

$$V_{min}^j \le V^j \le V_{max}^j \quad (22)$$

$$I_{GSC_i}^{rms} \le I_{GSC}^{rated} \quad (23)$$

$$\beta_{min} \le \beta_k \le \beta_{max} \quad (24)$$

$$0 \le P_{ref}^k \le P_{rated} \quad (25)$$

$$\frac{\partial C_P(\beta,\lambda)}{\partial \lambda} \le 0 \quad (26)$$

$$\frac{\partial C_P(\beta,\lambda)}{\partial \beta} \le 0 \quad (27)$$

where P_j and Q_j are the active power and reactive power injected at bus j, V^j and δ^j are the voltage and angle of each bus, Y_{ji} is the entry in the jth row i^{th} column of the admittance matrix, Q_{ref}^{WF} is the reactive power reference of the WF, I_{GSC}^{rated} is the rated current of the Grid Side Converter (GSC), The optimization variables used here are active power reference P_{ref}^k and reactive power reference Q_{ref}^k of each WT.

The constraints include the power flow balance limits (19), (20), the WF reactive power constraint (21), the bus voltage limit (22), the current constraint of the GSC (23), which is used to limit the reactive power, the pitch angle limit (24), the active power limit (25), and the WT operation region constraints (26), (27). In the power flow problem, the point of common coupling is treated as slack bus and all the other buses are treated as PQ buses. A full Newton–Raphson method is used to solve the power flow equations. Since the problem is nonlinear and non-convex, the PSO algorithm [34] is adopted to solve the optimization problem.

IV.   CASE STUDY

In this paper, the chosen WF has 5 rows, 5 turbines each row, with 882 m (seven times the WT diameter) between the turbines. The layout of the WF is shown in Fig. 1. The cables in the WF are XLPE-Cu and operated at 34 kV nominal

voltage. The parameters are shown in Table I. The WT parameters are shown in the appendix.
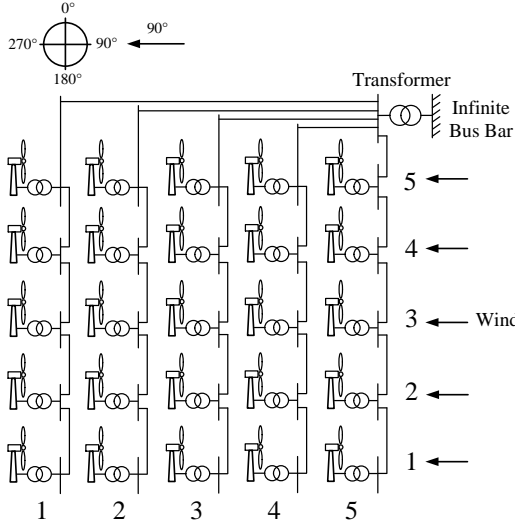

Fig. 1. The layout of the wind farm

TABLE I.
PARAMETERS OF CABLES [35]

Cross section mm2	Resistance Ω /km	Capacitance μF/km	Inductance mH/km
95	0.1842	0.18	0.44
150	0.1167	0.21	0.41
240	0.0729	0.24	0.38

There strategies are compared in this paper. Strategy A uses traditional WT active power control strategy (maximum power tracking) and traditional WF reactive power dispatch strategy (proportional distribution). Strategy B uses improved WF active power dispatch strategy (maximizing the captured power by derating the upwind WTs) and optimal reactive power dispatch strategy (optimal dispatch to minimize the active power loss). Strategy C uses coordinated WF active and reactive power dispatch strategy (maximizing the total output active power considering all the losses).

The strategies are compared when Q_{ref}^{WF} is 0.3 pu and wind directions are 90° and 270°. After 10 times simulation using PSO, the values are averaged and the results are shown in TABLE II.

TABLE II
COMPARISION OF THESE STRETEGIES AT DIFFERENT OPERATION CONDITIONS

Wind direction	Strategy	Output Power (MW)	Total loss (MW)	Cable loss (MW)	WT loss (MW)
90°	Strategy A	49.59	2.49	0.21	2.28
	Strategy B	52.23	2.45	0.23	2.22
	Strategy C	52.29	2.44	0.22	2.21
270°	Strategy A	49.53	2.56	0.27	2.28
	Strategy B	52.27	2.50	0.26	2.23
	Strategy C	52.33	2.47	0.26	2.21

It can be seen that using Strategy C, the WF output power is increased and the WT loss is reduced. The cable loss is increased at direction 90°, whereas it decreased at direction 270°. The reason is that the cable loss is related to the power circulation distance along the cables, and when wind direction is 90°, the WT produce more power is nearer to the PCC, so the power circulation distance is less than the solutions where upwind WTs are derated. However, the total loss is reduced because the WT loss decrease is more than the cable loss increase.

V. CONCLUSION

The coordinated active power and reactive power dispatch strategy proposed in this paper shows the potential to improve the output power of a WF. Comparing with the traditional active power and reactive power dispatch strategy, the loss reduction of an optimized dispatch strategy depends on if the loss model is accurate and complete, also depends on the wind direction, i.e., the original active power distribution pattern. Models of all the devices should be considered in the objective function. Otherwise, reducing losses in part of the devices will increase the losses in the other part. The cable loss is related to the wind directions, so it may be increased at some wind directions. The proposed dispatch strategy can be used in WF energy management systems or wind power dispatch centers.

APPENDIX

A. Wind Turbine

The 5 MW NERL WT is adopted as the reference WT [36]. The parameters are as follows:

TABLE III
NERL 5MW WIND TURBINE SPECIFICATION [36]

Parameter	5 MW NERL Wind Turbine
Cut-in, Rated, Cut-out Wind Speed	3 m/s, 11.4 m/s, 25m/s
Rotor, Hub Diameter	126 m, 3m
Rated Power	5 MW
Cut-In, Rated Rotor Speed	6.9 rpm, 12.1 rpm

B. Converters

The converters are chosen based on the method in [30]. Two IGBT modules (ABB 5SNA 2000K451300) are series connected on each bridge. Based on the data for the IGBT module on the data sheet [37], the power module constants $a_l = 7.0252$ and $b_l = 0.0087$, and f_{sw} is chosen as 800 Hz.

C. Transformer

The Siemens GEAFOL cast-resin transformer rated at 8000kVA is chosen as the transformer set in the WT, with no-load loss of 13.5 kW and load loss of 36 kW [38].

D. PMSG[30]

TABLE IV
PMSG PARAMETER

Parameter	Value
Rated Output Power (kW)	5000
Number of Poles	8
Frequency (Hz)	50
Armature Phase Resistance (Ohm)	0.0375
D-Axis Main Reactance (Ohm)	2.93

Q-Axis Main Reactance (Ohm)	2.93
Fundamental Induced Stator Line Voltage (Vrms)	5032.09
Stator Phase Current (Irms)	742.962
Power Factor	0.809748
Rated Rotational Speed (rpm)	750

REFERENCES

[1] Barthelmie R, Frandsen S, Hansen K, Schepers J, Rados K, Schlez W, Neubert A, Jensen L, Neckelmann S. Modelling the impact of wakes on power output at Nysted and Horns Rev. Proceedings of the European Wind Energy Conference, Marseille, France, 2009.

[2] Jiménez Á, Crespo A, Migoya E. Application of a LES technique to characterize the wake deflection of a wind turbine in yaw. Wind Energy 2010; 13(6): 559–572.

[3] Fleming PA, Gebraad PMO, Lee S, van Wingerden JW, Johnson K, Churchfield M, Michalakes J, Spalart P, Moriarty P. Evaluating techniques for redirecting turbine wakes using SOWFA. Renewable Energy 2014; 70: 211–218.

[4] Fleming P, Gebraad PMO, Lee S, van Wingerden JW, Johnson K, Churchfield M, Michalakes J, Spalart P, Moriarty P. Simulation comparison of wake mitigation control strategies for a two-turbine case. Wind Energy 2014.

[5] P. M. Gebraad, F. W. Teeuwisse, J.-W. van Wingerden, P. Fleming, S. D. Ruben, J. R. Marden, and L. Y. Pao, "Wind plant power optimization through yaw control using a parametric model for wake effects - a CFD simulation study," Wind Energy, vol. 17, pp. 657–669, 2014.

[6] J. R. Marden, D. R. Shalom, L.Y. Pao, "A model-free approach to wind farm control using game theoretic methods," *IEEE Trans. Control Syst. Technol.*, vol. 21, no. 4, pp. 1207–1214, July 2013.

[7] P. M. O. Gebraad, and J. W. Wingerden, "Maximum power point tracking control for wind farms," *Wind Energy*, vol. 18, pp. 429–447, 2015.

[8] J. P. Goit and Meyers J, "Analysis of turbulent flow properties and energy fluxes in optimally controlled wind-farm boundary layers," in *The science of making torque from wind*, Lyngby, Denmark, 2014.

[9] T. Horvat, V. Spudić, M. Baotić, "Quasi-stationary optimal control for wind farm with closely spaced turbines," in *MIPRO, 2012 Proceedings of the 35th International Convention*, Opatija, 2012, pp. 829–834.

[10] J. Park, S. Kwon, and K. H. Law, "Wind farm power maximization based on a cooperative static game approach," in *Proceedings of the SPIE active and passive smart structures and integrated systems conference*, San Diego, CA, USA, 2013.

[11] J. Lee, E. Son, B. Hwang, et al, "Blade pitch angle control for aerodynamic performance optimization of a wind farm," *Renew. Energy*, vol. 54, pp. 124–130, 2013.

[12] A. Behnood, H. Gharavi, B. Vahidi, et al, "Optimal output power of not properly designed wind farms, considering wake effects," *Int. J. of Electric. Power & Energy Syst.*, vol. 63, pp. 44–50, 2014.

[13] J. S. González, M. B. Payán, J. R. Santos, et al, "Maximizing the overall production of wind farms by setting the individual operating point of wind turbines," *Renewable Energy*, vol. 80, pp. 219–229, 2015.

[14] B. Zhang, W. Hu, P. Hou, et al, "Wind Farm Active Power Dispatch for Output Power Maximizing Based on a Wind Turbine Control Strategy for Load Minimizing," presented in SMART 2015.

[15] M. Mirzaei, M. Soltani, N. K. Poulsen, et al, "Model based active power control of a wind turbine," in 2014 *American Control Conference (ACC)*, Portland, Oregon, 2014, pp. 5037–5042.

[16] A. Tapia, G. Tapia, J. X. Ostolaza, "Reactive power control of wind farms for voltage control applications", *Renewable Energy*, vol. 29, pp. 377‑392, 2004.

[17] Y. Lang, X. Zhang, D. Xu, et al, "Reactive Power Analysis and Control of Doubly Fed Induction Generator Wind Farm," *Proc. of the CSEE*, vol. 27, no.9, Mar. 2007.

[18] J. R. Saenz, A. Tapia, G. Tapia, et al, "Reactive power control of a wind farm through different control algorithms," in *Proc. of the 4th IEEE Int. Conf. on Power Electron. and Drive Syst.*, Denpasar, 2001, pp. 203–207.

[19] B. Kanna, S. N. Singh, "Towards reactive power dispatch within a wind farm using hybrid PSO," *Int. J. of Elect. Power & Energy Syst.*, vol. 69, pp. 232–240, 2015.

[20] M. Martinez-Rojas, A. Sumper, O. Gomis-Bellmunt, et al, "Reactive power dispatch in wind farms using particle swarm optimization technique and feasible solutions search," *Applied Energy*, vol. 88, no. 12, pp. 4678–4686, 2011.

[21] B. Zhang, W. Hu, P. Hou, et al, "Reactive power dispatch for loss minimization of a doubly fed induction generator based wind farm," in *IEEE 17th Int. Conf. on Elect. Mach. and Syst.*, Hangzhou, China, 2014, pp. 1373-1378.

[22] R. G. De Almeida, E. D. Castronuovo, J. A. Peas Lopes, "Optimum generation control in wind parks when carrying out system operator requests," *IEEE Trans. Power Syst.*, vol. 21, no. 2, pp. 718–725, May 2006.

[23] Moyano, Carlos F., and Joao A. Pecas Lopes. "An optimization approach for wind turbine commitment and dispatch in a wind park." Electric Power Systems Research 79.1 (2009): 71-79.

[24] V. Spudić, M. Jelavić, M. Baotić, "Wind turbine power references in coordinated control of wind farms," *Automatika–J. for Control, Measurement, Electron., Computing and Commun.*, vol. 52, no. 2, pp. 82–94, 2011.

[25] Roshanfekr P, Thiringer T, Alatalo M, et al. Performance of two 5 MW permanent magnet wind turbine generators using surface mounted and interior mounted magnets[C]//Electrical Machines (ICEM), 2012 XXth International Conference on. IEEE, 2012: 1041-1047.

[26] A. D. Hansen., C. Jauch, P. Sørensen, et al, "Dynamic wind turbine models in power system simulation tool DIgSILENT," Tech. Rep. Risø-R-1400, Risø, Roskilde, Denmark, 2003.

[27] F. González-Longatt, P. Wall and V. Terzija, "Wake effect in wind farm performance: Steady-state and dynamic behavior," *Renewable Energy*, vol. 39, pp. 329–338, Sep. 2011.

[28] F. Port´e-Agel, Y. Wu, C. Chen, "A Numerical Study of the Effects of Wind Direction on Turbine Wakes and Power Losses in a large Wind Farm," *Energies*, vol. 6, pp. 5297–5313, MDPI, 2013.

[29] Chinchilla, Monica, Santiago Arnaltes, and Juan Carlos Burgos. "Control of permanent-magnet generators applied to variable-speed wind-energy systems connected to the grid." Energy Conversion, IEEE Transactions on 21.1 (2006): 130-135.

[30] Roshanfekr, Poopak, et al. "Selecting IGBT module for a high voltage 5 MW wind turbine PMSG-equipped generating system." Power Electronics and Machines in Wind Applications (PEMWA), 2012 IEEE. IEEE, 2012.

[31] A. Petersson, "Analysis, modeling and control of doubly-fed induction generators for wind turbines," Ph.D. dissertation, Dept. Energy and Environment, Chalmers Univ. of Tech., Goteborg, Sweden, 2005.

[32] Siemens Energy Sector. *Transformers (7th Ed.)* [Online]. Available: http://www.energy.siemens.com/hq/pool/hq/power-transmission/Transformers/downloads/peg-kapitel-5.pdf

[33] H. Saadat, *Power System Analysis*. New York: McGraw-Hill, 1999, pp. 189–219.

[34] M. Clerc, J Kennedy, "The particle swarm – explosion, stability, and convergence in a multidimensional complex space," *IEEE Trans. Evol. Comput.*, vol. 6, no. 1, pp. 58–73, 2002.

[35] ABB. *XLPE Submarine Cable Systems* [Online]. Available: http://www05.abb.com/global/scot/scot245.nsf/veritydisplay/2fb009430 6e48975c125777c00334767/$file/XLPE%20Submarine%20Cable%20S ystems%202GM5007%20rev%205.pdf

[36] J. Jonkman, S. Butterfield, W. Musial, et al, "Definition of a 5-MW Reference Wind Turbine for Offshore System Development," CO: NREL, Golden, Tech. Rep. NREL/TP-500-38060, Feb. 2009.

[37] ABB Switzerland Ltd. (2013, Jan.). 5SNA 2000K451300, StakPak IGBT Module. Lenzburg, Switzerland. [Online]. Available: http://new.abb.com/semiconductors/insulated-gate-bipolar-transistor-(igbt)-and-diode-modules/stakpak.

[38] Siemens AG. (2007). GEAFOL cast-resin transformer 100 to 16000 kVA. Kirchheim/Teck, Germany. [Online]. Available: http://www.energy.siemens.com/br/pool/br/tran

smissao-de-energia/transformadores/geafol-2010_Eng.pdf